Hybrid Conversion of 5 -Hydroxymethylfurfural to 5 -Aminomethyl- 2 -furancarboxylic acid: Toward New Bio-sourced Polymers

Antoine Lancien, Robert Wojcieszak, Eric Cuvelier, Matthieu Duban, Pascal Dhulster, Sébastien Paul, Franck Dumeignil, Renato Froidevaux, Egon Heuson

ChemCatChem

The European Society Journal for Catalysis

Chemistry Europe

European Chemical Societies Publishing

Cover Feature:

A. Lancien et al.

Hybrid Conversion of *5*-Hydroxymethylfurfural to *5*-Aminomethyl-*2*-furancarboxylic acid: Toward New Bio-sourced Polymers

Supported by GECATS German Catalysis Society

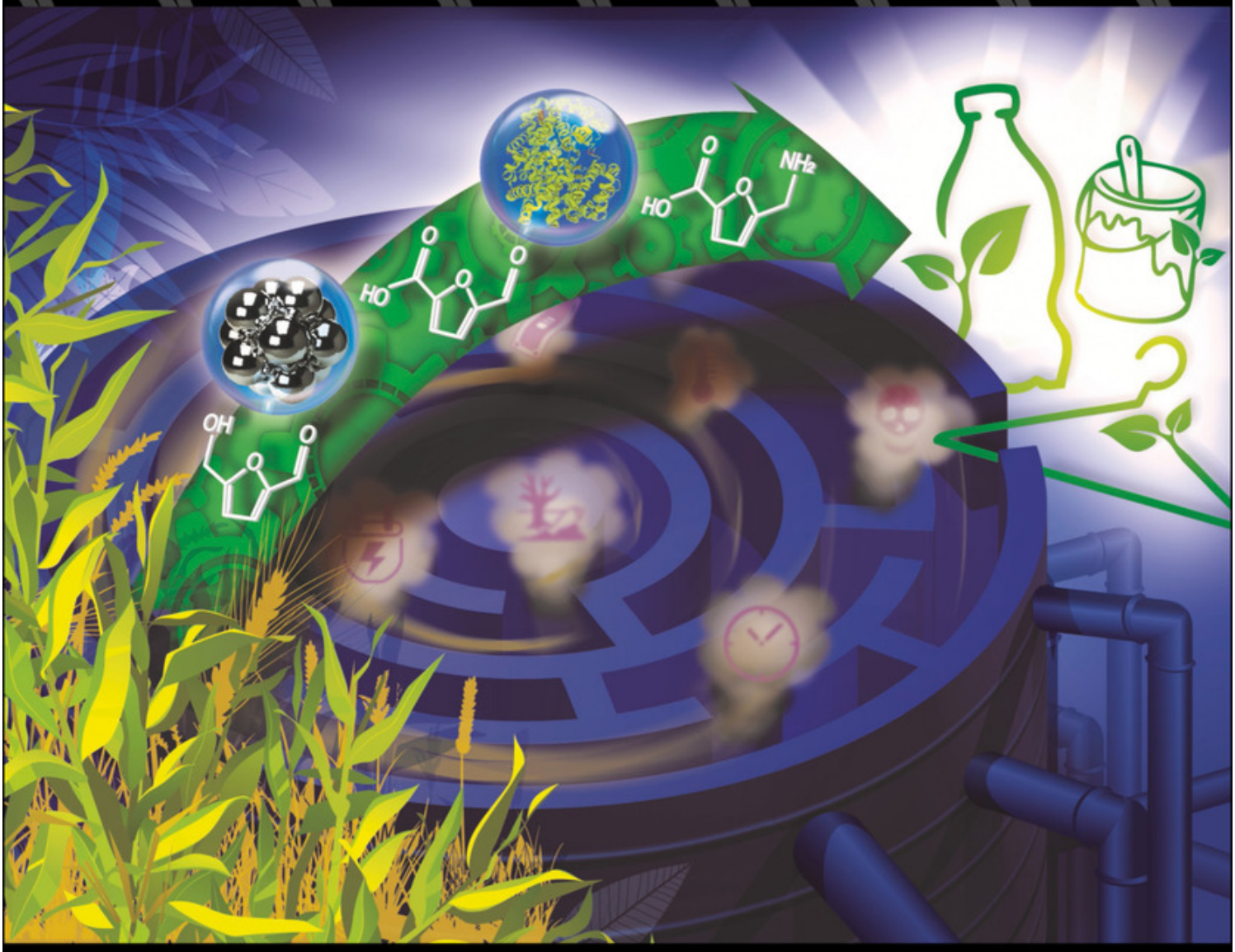

1/2021

WILEY-VCH

FULL PAPER

Hybrid conversion of *5*-hydroxymethylfurfural to *5*-aminomethyl-*2*-furancarboxylic acid: toward new bio-sourced polymers

Antoine Lancien,[a] Robert Wojcieszak,[b] Eric Cuvelier,[b] Matthieu Duban,[a] Pascal Dhulster,[a] Sébastien Paul,[b] Franck Dumeignil,[b] Renato Froidevaux*,[a] and Egon Heuson*,[a]

[a] A. Lancien, Dr. M. Duban, Prof. P. Dhulster, Prof. R. Froidevaux, Dr. E. Heuson
Univ. Lille, INRA, ISA, Univ. Artois, Univ. Littoral Côte d'Opale, EA 7394, Joint Research Unit BioEcoAgro – ICV- Institut Charles Viollette, F-59000 Lille, France
E-mail: egon.heuson@univ-lille.fr, renato.froidevaux@univ-lille.fr
Twitter : @egonheuson

[b] Dr. R. Wojcieszak, E. Cuvelier, Prof. S. Paul, Prof. F. Dumeignil
Univ. Lille, CNRS, Centrale Lille, Univ. Artois, UMR 8181 - UCCS - Unité de Catalyse et Chimie du Solide, F-59000 Lille, France
Twitter : @wojcieszakr, @UCCS_8181

Abstract: Hybrid catalysis, which combines chemo- and biocatalytic benefits, is an efficient way to address g*reen chemistry* principles. *5*-Hydroxymethylfurfural (HMF) is a versatile building block in numerous industrial applications. To date, few studies have described the production of its amine derivatives and their polymers. Finding a good methodology to directly transform HMF to *5*-aminomethyl-*2*-furancarboxylic acid (AMFC) therefore represents an important challenge. After selecting the best oxidation catalyst for HMF conversion to *5*-aldehyde-*2*-furancarboxylic acid and immobilizing a transaminase onto a solid carrier, we implemented the first one-pot/two-steps hybrid catalytic process to produce AMFC (77 % yield); this is the most efficient AMFC catalytic production method from HMF reported to date. This process also produced *2,5*-furandicarboxylic acid (21 % yield) as a major secondary product that can be applied to polymer syntheses such as polyethylene furanoate. Herein, we report a novel way to access new biosourced polymers based on HMF oxidized and aminated derivatives.

Introduction

The development of greener chemical processes is now recognized as a priority. The rarefaction of fossil resources combined with climate change issues impose the complete rethinking of our consumption habits and production models. Since the formalization of the concept of *green chemistry* by Anastas and Warner,[1] chemists have been looking for alternative syntheses that are more efficient, less energy consuming, economically sustainable, and more environmentally friendly. Catalytic processes can fulfill most of these requirements; however, they are traditionally based on the use of a single chemo- or biocatalyst, thus only enabling a relatively limited range of reactions. Multicatalytic cascade-type systems have also been studied, with numerous successful examples expending the scope of the achieved reactions. Still, they mostly concentrate on the same types of catalysts, namely chemo- and biocatalysts. Combining these two catalyst types would further expand the reaction variations. The number of studies reporting such combinations has recently increased and the variety of new accessible chemicals is continuously broadening.[2] This is especially observed in the synthesis of asymmetric compounds through different methodologies such as dynamic kinetic resolution processes.[3] Still, the industrial application of these reactions is often very limited owing to their difficulty of implementation. The main challenge lies in finding catalysts that do not inhibit each other and of more importance, in establishing operating conditions that retain the activity of both catalysts. To circumvent such issues, the catalysts are most often used in different successive steps,[4] or isolated from each other through compartmentalization *via* various methods including two-phase systems communicating through liquid/liquid or solid membranes[3b,5] and whole-cell encapsulation of one of the two catalysts.[6]

To address these catalyst combination issues, the novel research field *"hybrid catalysis"* has recently emerged. It involves the concomitant use of a chemo- and biocatalyst in a single pot, to realize multiple successive reactions.[7] Under one of its simplest forms, a hybrid catalytic reaction combines two soluble catalysts, usually comprising an organocatalyst + biocatalyst. The first examples of such a combination were reported in the early 2000s. In 2003, Schoevaart *et al.* combined *L*-proline as an organic chemocatalyst with a *D*-galactose oxidase and Pt/C hydrogenation catalyst and employed this hybrid catalyst in the synthesis of *4*-deoxy-*D*-glucose derivatives from *D*-galactose in a one-pot/three-steps process.[8] One year later, Edin *et al.* described the synthesis of enantiomerically pure acetylated aldols by combining aldolization with acetylation, catalyzed respectively by an *(S)*-proline and lipase.[9] These examples mainly established the compatibility between biocatalysts and some organocatalysts, subsequently leading to numerous other applications.[2c,2d,7] Heterogeneous chemo- and biocatalysts can also be advantageously combined; however, literature on such methods is scarce. The first example was reported in 1980 with the combination of a glucose isomerase and, once again, a Pt/C chemocatalyst applied for the preparation of *D*-mannitol.[10] Following these reports, a few successful examples of heterogenocatalytic hybrid pathways have been described where at least one of the two catalysts is supported on a solid carrier.[11] The heterogeneous hybrid approach offers the main advantage of considerably simplifying the purification processes by facilitating catalyst separation from the reaction medium.

The hybrid catalysis concept is particularly relevant in the context of biorefineries, with biomass as an alternative feedstock to

petroleum for production processes, *e.g.* chemicals,[12] with the catalytic production of a large number of compounds.[13] Among them, *5*-hydroxymethylfurfural (HMF) is described as one of the most important biobased platform molecules[14] with various production processes.[13c,15] A two-pots/one-step hybrid catalytic pathway was recently reported by Gimbernat *et al.* for HMF production from *D*-glucose in a triphasic compartmentalized reactor.[5a]

This product can be transformed into a variety of value-added building blocks,[16] including monomers useful for the production of biosourced polymers such as *2,5*-dihydroxymethylfuran (DHMF), *2,5*-dicarboxaldehydefuran (DCAF), *5*-hydroxymethyl-*2*-furancarboxylic acid (HFCA), and *2,5*-furandicarboxylic acid (FDCA; Figure 1), with a wide range of innovative approaches.[17] HMF transformation in FDCA for example has been investigated intensively through last decades and many approaches have been reported.[17b, 18] Chemical catalysts based on noble-metal materials showed high activity in HMF oxidation.[19] Supported noble metal nanoparticles have shown superior catalytic activity in the liquid phase oxidation of HMF in both, alkaline and acidic conditions.[20] Moreover, enzymes were also applied. One of the first studies that reported biological systems for the oxidation of HMF was that of Koopman who identified a novel HMF oxidoreductase from *Cupriavidus basilensis* HMF14. The hmfH gene encoding was introduced into *Pseudomonas putida* S12, and the resulting whole cell biocatalyst was used to produce FDCA from HMF. In fed-batch experiments using glycerol as the carbon source, 30.1 $g.L^{-1}$ of FDCA were produced from HMF with a yield of 97 %.[21] Dijkman et al. identified and applied the HMF oxidase (expressed on *E. coli* BL21 (DE3)) to obtain FDCA from HMF in 4 steps. This FAD-dependent enzyme was able to express more than 95 % of conversion in 24 h at 25 °C with 4 mM HMF, 20 mM HMFO, and 20 mM FAD in a 100 mM PBS solution with pH 7.[22] Carro et al. applied unspecific aryl-alcohol oxidase (AAO) from *Agrocybe aegerita* in a reaction cascade to transform HMF to FDCA. AAO provided H_2O_2 from O_2 reduction and could stepwise oxidize HMF to DFF (2,5-diformylfuran) and further to FFCA (5-formylfuran-2-carboxylic acid). However, the enzyme was unable to oxidize the carbonyl groups in FFCA, but could catalyze the oxidation of FFCA to FDCA using H_2O_2 as a co-substrate, achieving a yield of 91 % FDCA after 116 h.[23] A tandem oxidation reaction to FDCA from HMF through a combination of galactose oxidase from *Dactylium dendroides*, horseradish peroxidase, and lipase was investigated by Zong et al., where a conversion of 75 % of HMF to DFF was achieved in 48 h at room temperature. DFF was further converted to FDCA due to reaction catalyzed by immobilized lipase B from Candida antarctica and H_2O_2, generating 88 % yield of FDCA after 24 h, and 92 % after 92 h.[24] The coupling of strategic oxidases in enzymatic cascade reaction to FDCA was also the main topic of the work of Mc Kenna et al, that applied *Escherichia coli* periplasmic aldehyde oxidase PaoABC and galactose oxidase M3-5. In the process more than 99 % FDCA yield was achieved in 16 h.[25] Liu and coworkers applied immobilized Laccase on magnetic nanoparticles with TEMPO as mediator, obtaining a FDCA yield of 90.2 % in 96 h at 35 °C.[26]

With the same mindset, furfurylamines have also been described as interesting precursors for biobased polymers including polyamides, polyimides, polyaspartimides, polyureas, polyhydroxyurethanes, polyimines, and polyenamines, with their monomers being readily synthesized from biosourced furfural derivatives.[27] These compounds also have several applications including the preparation of benzoxazine derivatives for flame-retardant resins[28] and, after conversion to difurfuryl diisocyanates, the replacement of petroleum-based diphenylmethane diisocyanate in polyurethane systems.[29]

Furfurylamines are most commonly obtained *via* the reductive amination of the carbonyl moiety of the furfural group,[30] under mild conditions with inexpensive reagents. However, such processes often require the use of protecting groups, numerous chemical steps, and toxic reductive agents.[30,31] To circumvent these issues, several chemocatalytic pathways have been recently developed;[30,31,32] however, these are not ideal for the synthesis of furfurylamines deriving from HMF, owing to the sensitivity of the furan ring to reductive conditions and the tendency of these compounds to form secondary and tertiary amines.[17,32g,33] An efficient alternative to perform reductive amination of HMF derivatives is the use of transaminases, already largely described for carbonyl group amination,[34] for the efficient conversion of carbonyl moieties to primary amines in water at low temperatures. Recently, several *ω*-transaminases were employed for the synthesis of several furfurylamines from HMF derivatives.[33,35] Dunbabin *et al.* reported yields ≤92 % for the aminated products, starting from different HMF and furfural derivatives. Among them, they achieved the synthesis of *5*-hydroxymethylfurfurylamine (HMFA), *5*-aminomethyl-*2*-furancarboxaldehyde (AMFA), furan-*2,5*-diyldimethanamine (FDMA), and *5*-aminomethyl-*2*-furancarboxylic acid (AMFC; Figure 2). However, in the case of AMFC, they performed the synthesis directly on *5*-aldehyde-*2*-furancarboxylic acid (AFCA) instead of HMF, owing to the absence of a prior oxidation step for the production of this intermediate in the reaction medium. Evidently, the only amine that can be directly produced from HMF is HMFA.

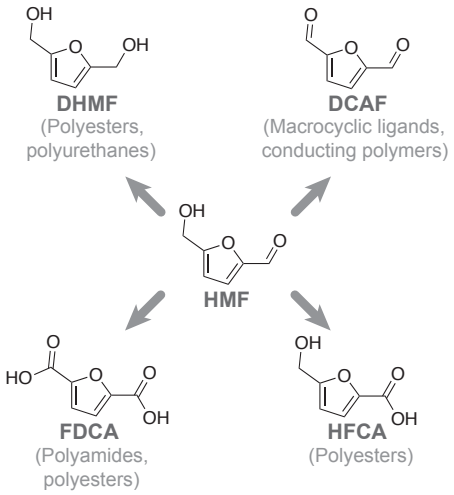

Figure 1. Valorization of *5*-hydroxymethylfurfural (HMF) into *2,5*-dihydroxymethylfuran (DHMF), *2,5*-dicarboxaldehydefuran (DCAF), *5*-hydroxymethyl-*2*-furancarboxylic acid (HFCA), and *2,5*-furandicarboxylic acid (FDCA) as building blocks for biobased polymers (applications indicated in brackets).

The synthesis of AMFA, FDMA, and AMFC requires a prior oxidation step to yield an aldehyde or carboxylic acid group from the hydroxyl moiety. For FDMA, the double aminated compound, this step should be preferably performed prior to the transaminase

action as the two carbonyls could then be converted concomitantly by the enzyme. While HMFA has proven to be useful for several applications (such as the preparation of diuretics, antihypertensives, and antiseptic and curing agents), AMFA and AMFC are very promising building blocks for polymer synthesis, owing to the presence of the aldehyde and carboxylic acid groups. AMFA can be used to form imine-based polymers based on a self-condensation mechanism, while AMFC, as an amino acid, can be used to produce unnatural peptides such as cyclopeptides.[36] These compounds are of great interest because of their considerable bioactivity. Surprisingly, very few studies have reported the successful synthesis of these two compounds and thus, finding a methodology to produce them in larger quantities would certainly help develop their use in polymer synthesis. Herein, we report the first combination of an oxidative metal chemocatalyst and a transaminase, as a heterogeneous hybrid catalytic one-pot/two-steps process, for the successful synthesis of AMFC from HMF (Figure 3). This strategy is based on a first step comprising the oxidation of HMF into AFCA by the chemocatalyst to generate the substrate required for the following transamination step to produce AMFC using an amine donor. The choice of a hybrid system, using a chemocatalyst instead of an enzyme, was motivated by the ability of our catalyst to directly use molecular oxygen for the oxidation step instead of an expensive cofactor/co-substrate, despite the complexity of making these two catalysts work in the same reaction mixture. Therefore, such a system should be more easily transposable to industrial considerations. The first realization of this innovative process ended in the complete conversion of HMF in 52 h to produce AMFC in 77 % yield. Additionally, FDCA was produced as major byproduct with a yield of 21 %.

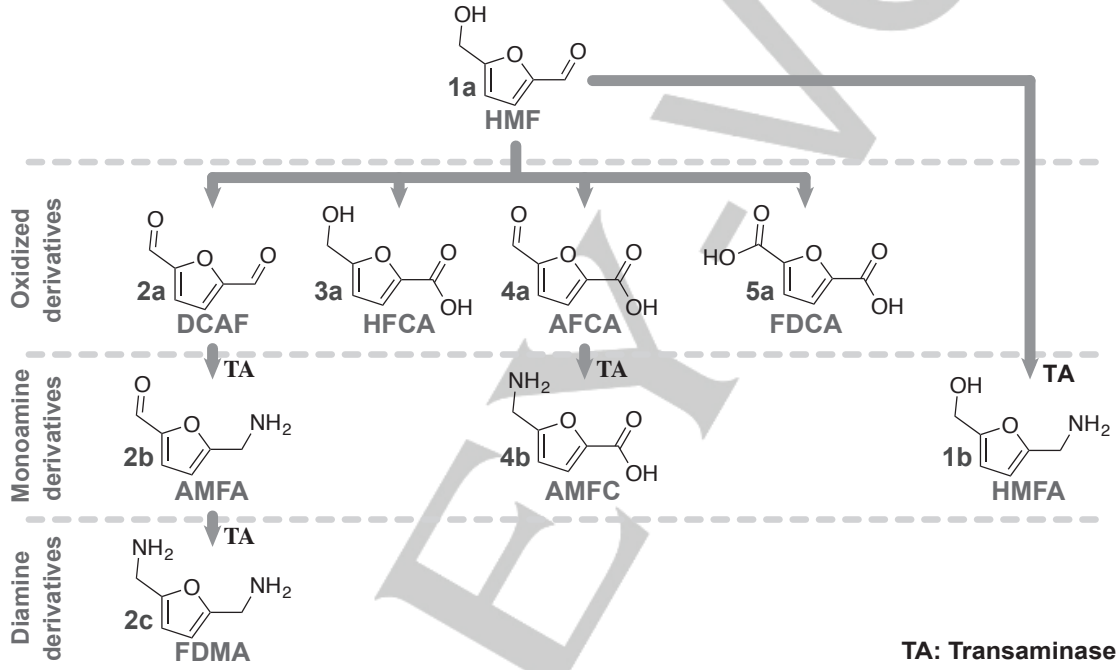

Figure 2. Chemical compounds obtained from: *1)* oxidation of the hydroxyl and carbonyl groups of *5*-hydroxymethylfurfural (HMF, **1a),** *2,5*-dicarboxaldehydefuran (DCAF, **2a**), *5*-hydroxymethyl-*2*-furancarboxylic acid (HFCA, **3a**), *5*-aldehyde-*2*-furancarboxylic acid (AFCA, **4a**), and *2,5*-furandicarboxylic acid (FDCA, **5a**)] and *2)* reductive amination of the corresponding carbonyl derivatives [*5*-hydroxymethylfurfurylamine (HMFA, **1b**), *5*-aminomethyl-*2*-furancarboxaldehyde (AMFA, **2b**), *5*-aminomethyl-*2*-furancarboxylic acid (AMFC, **4b**), and furan-*2,5*-diyldimethanamine (FDMA, **2c**)]. Some of these reductive aminations were recently performed with enzymes, especially with transaminases (TA), in one-step reactions, helping for the development of greener processes.

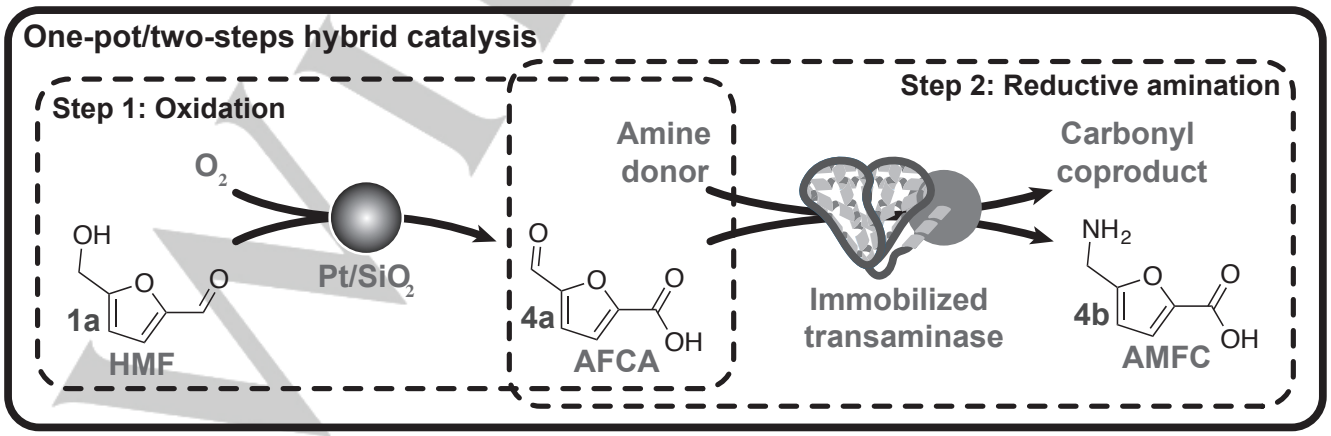

Figure 3. One-pot/two-steps hybrid catalytic process for the direct synthesis of *5*-aminomethyl-*2*-furancarboxylic acid (AMFC) from *5*-hydroxymethylfurfural (HMF) combining a heterogeneous metal oxidative catalyst and an immobilized transaminase.

Only traces (<1 %) of HFCA could be detected at the end of the process, proving its efficiency for the synthesis of biobased polymer precursors. Notably, respective AMFC and FDCA yields of 67 and 20 % could by recovered after purification without further optimization.

Results and Discussion

Chemocatalyst screening

To achieve the conversion of **1a** to **4b**, the reaction pathway must first proceed through the production of **4a** under a first oxidation step. The oxidative metal catalysts were therefore first screened on **1a** to evaluate their ability to produce **4a** selectively at 60 °C in a phosphate buffer at pH 8, the conditions required for transaminase activity during the second step of the reaction, with sole molecular oxygen as the oxidant. In total, 15 heterogeneous metal catalysts were screened on **1a** at small scale (1 mL), in glass sealed vials, to limit evaporation. The tested catalysts, which were selected according to their ability and versatility to oxidize short-chain alcohols are listed in Table 1.[28b, 37]

Table 1. Oxidation catalysts screened for the conversion of **1a** to **4a**.

Catalyst code name	Method of preparation	Metal content (ICP)	Support
C1	Reduction-precipitation	2.3 % Au	Al_2O_3
C2	Sol immobilization	1.8 % Au	Amberlyst 15
C3	Sol immobilization	1.6 % Au	CaO
C4	Sol immobilization	1.6 % Au_{PVA}	CaO
C5	Sol immobilization	1.8 % Au	CeO_2
C6	Sol immobilization	1.8 % Au	MgO
C7	Reduction-precipitation	1.7 % Pd	Al_2O_3
C8	Sol immobilization	0.9 % Pd	TiO_2
C9	Wet impregnation	6.3 % Pt	SiO_2
C10	Wet impregnation	1.5 % Ru	$Ca_{10}(PO_4)_6(OH)_2$
C11	Sol immobilization	0.9 % Au – 0.1 % Pd	TiO_2
C12	Sol immobilization	0.3 % Au – 0.7 % Pd	ZrO_2
C13	Co-precipitation	0.8 % Au – 0.8 % Pt	TiO_2
C14	Co-precipitation	0.7 % Pt – 0.8 % Pd	Al_2O_3
C15	Co-precipitation	1.0 % Pt – 1.0 % Pd	TiO_2

The catalytic test results are presented in Figure 4. The results revealed that the 7.68 µmol O_2 contained in the 1 mL gas phase were sufficient to oxidize **1a** over several catalysts. As a result, catalysts C1, C3, C5, C8, C13, C14, and C15 were found inactive, while the rest of the catalysts formed at least one oxidation product: **3a**, **4a**, and/or **5a** (Figure 4). Interestingly, no **2a** could be detected despite it being one of the first two oxidative products of **1a**. Catalysts C4, C6, C7, and C11 afforded 8.0, 9.0, 1.5, and 4.8 mM of **3a**, respectively, after 24 h. On the other hand, despite the complete conversion of **1a** with C4 and C6, these two catalysts afforded low amounts of **4a** at the concentrations 0.8 and 0.9 mM. Similar concentration levels were obtained with C7 and C11, with 0.5 and 0.9 mM respectively. This suggests that under the proposed conditions, these catalysts favor the conversion of the aldehyde **1a** to a carboxylic acid moiety over that of the alcohol to an aldehyde moiety, which here remains the limiting step. This was confirmed by the concomitant production of **5a** and **4a** with C4 and C6 at the concentrations 0.7 and 0.2 mM, respectively. Consequently, while the amount of **4a** produced was significant, C4 and C6 were considered poor candidates for the cascade reaction, as the yield of the second step would remain limited under these conditions, even with the complete consumption of **1a**. In contrast, C2, C10, and C12 selectively led to **4a** at the respective concentrations 0.5, 0.7, and 0.7 mM. This suggested that for these catalysts, the limiting step was the conversion of the aldehyde group into carboxylic acid, thereby leading to the straightforward conversion of **3a** to **4a**. Still, the very low amount of **4a** produced in 24 h was not encouraging. The most efficient catalyst for the production of **4a** was Pt/SiO_2 (C9), with full conversion of HMF after 24 h and the production of 8.1 and 2.0 mM **4a** and **5a**, respectively. The absence of **3a** suggests a reaction pathway similar to that observed over C2, C10, and C11, with conversion of the aldehyde into the acid as the limiting step. With a yield of **4a** of >80 % after 24 h, C9 was selected for the subsequent hybrid process.

Transaminase activity towards the potential oxidized products

The activity of *Chromobacterium violaceum* transaminase (*Cv*-TA) toward the different potential substrates present in solution was next evaluated using a lactate dehydrogenase (LDH) assay based on alanine as the amine donor for transamination.[38] This led to the production of pyruvate as a carbonyl co-product, which was subsequently reduced to the lactate by LDH with a molecule of NADH. The conversion of this latter molecule to NAD^+ was detected by UV spectrophotometry at 340 nm (ε_{340nm} = 6220 $M^{-1}.cm^{-1}$, pH 8), which thus allowed the determination of the reaction advancement. First, the activity of *Cv*-TA toward **1a** was measured to assess its possible competition with the chemocatalyst used to produce **4a**. Such a transamination reaction would lead to the production of **1b**, which may not be oxidized by the chemocatalyst and would thus result in a decrease in the yield of **4b**. An activity of 10.7 mUI.well^{-1} was observed, indicating a specific activity of 535 mUI.mg^{-1} of cell-free extract (CFE). The activity towards **4a**, the intermediate compound of the hybrid reaction, was then investigated under the same conditions. Thus, 14.3 mUI.well^{-1} (715 mUI.mg^{-1} CFE) was measured with the LDH assay. Finally, the ability of the transaminase to accept **2a** as a substrate was also evaluated. Here, 10.9 mUI.well^{-1} was measured for this substrate, leading to a specific activity of 545 mUI.mg^{-1} *Cv*-TA CF

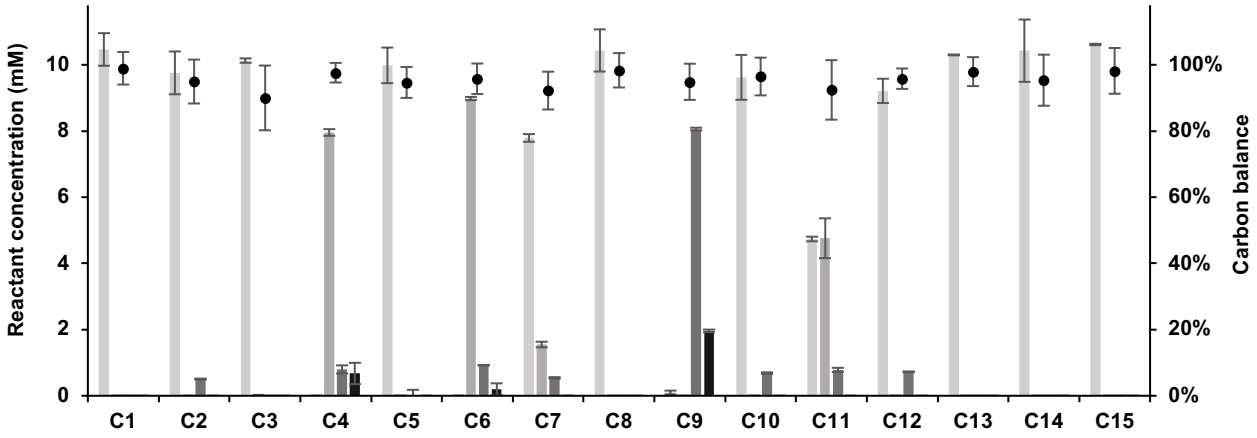

Figure 4. Concentrations of **1a**, **3a**, **4a**, and **5a** measured by high-performance liquid chromatography with diode-array detection (HPLC-DAD) after reaction for 24 h, at 60 °C, over the 15 selected chemocatalysts. The screening was performed in 1 mL of 100 mM sodium phosphate buffer (pH 8) in ultra-pure water on 10 mM 1a, with 2 mg chemocatalyst. Carbon balances (•) were calculated for each catalyst

To fit the experimental conditions previously defined during the chemocatalysis screening step, the activity of *Cv*-TA toward **4a** at 60 °C was next investigated. The results revealed that 43 % **4a** was converted at 60 °C in 90 min, while 62 % conversion of **4a** to **4b** was achieved in 90 min at 30 °C (Figure SI 1). Notably, this low yield was probably due to the absence of equilibrium shifting methodology application in this assay, as LDH was only added after sampling because of its instability at 60 °C. The final yield therefore reflects the equilibrium constant of the reaction for these substrate couples. The rapid formation of a blurry precipitate was also observed in the mixture at 60 °C suggesting enzyme precipitation, while no precipitate was observed at 30 °C.

Following the evaluation of *Cv*-TA activity toward the different substrates of the reaction, the synthesis of **4b** from **4a** was performed at small scale to evaluate the ability of the enzyme to successfully convert the intermediate of the final hybrid reaction. Notably, this synthesis was already described by Dunbabin *et al.* with several TAs,[33] including *Cv*-TA, using methylbenzylamine (MBA) and *iso*propylamine (IPA) as the amine donors. These two donors are known to shift the reaction equilibrium. In their study, Dunbabin *et al.* reported 47 and 88 % yields for the transamination of **4a** to **4b** with both donors, respectively. In this study, we performed these tests on the **4a** acceptor using both MBA and IPA donors. Although MBA presents a molecular weight equivalent to our desired product, a 1:1 ratio with the **4a** acceptor was used to fulfill at best the principles of *green chemistry*. With the *Cv*-TA being strictly *(S)*-enantioselective, *(S)*-MBA was used as the pure enantiomer in this study. The reaction led to the quantitative production of **4b** in 5 h. This demonstrates the *Cv*-TA efficiency in producing **4b** under these conditions. With IPA, a 1:1 ratio was also first tested; however, the conversion yield remained low (<7 %) after 4 h of transamination (Figure SI 2). Thus, a 100:1 ratio was next tested, and the quantitative production of **4b** could be observed in only 4 h under these conditions. While this high donor/acceptor ratio is commonly reported throughout the literature for transaminase synthesis with IPA, we are fully aware that using such an amount of donor does not respect the principles of *green chemistry*. Therefore, as will be described later in this study, when using IPA as donor, our processes used a 10:1 donor/acceptor ratio to head in this direction. Under such conditions, a quantitative production of **4b** could also be achieved. Because they are not commercially available, the syntheses of **1b** and **2b** by the transamination of the corresponding carbonyls (**1a** and **2a**, respectively) were also tested to serve as reference compounds for the HPLC analysis. In this case, sole MBA was used as the donor in a 1:1 ratio. Compound **1b** could be obtained quantitatively from **1a**. For **2b** production, the product could not be purified after the reaction was terminated. However, the HPLC data revealed complete conversion of **2a** in 2 h, leading to the production of an amine product that was assumed to be **2b**. Interestingly, a small quantity of a second amine product was also detected. Considering that **2a** possesses two carbonyl moieties, we assumed that this second compound was probably **2c**. However, because the production of **2a** was not detected during the chemocatalyst screening, no production of **2b** and **2c** was expected during the hybrid catalytic synthesis. Thus, no further syntheses of these two standards were attempted.

Cv-TA immobilization

The immobilization of *Cv*-TA was then performed on a solid carrier. For this purpose, we selected the EziG™ carrier (EnginZyme AB, Sweden), which was described in 2014 by Cassimjee et al. as an efficient immobilization support for *Cv*-TA with higher stability in organic solvents.[39] The use of this carrier was very recently extended to several other enzyme classes by Thompson *et al.*.[40] This carrier is available under three different forms with three different polymer coatings, namely, the EziG™ hydrophilic OPAL, semi-hydrophilic AMBER, and hydrophobic CORAL. Thus, to select the most efficient carrier for the enzyme, all forms were tested. The *Cv*-TA was immobilized directly from the CFE in the presence of a slight amount of its cofactor, pyridoxal phosphate (PLP), to maintain a good folding of the enzyme. Interestingly, after the immobilization and washing steps, the carrier turned yellowish, even when no CFE was used, suggesting a strong affinity for PLP.

First an evaluation of the best enzyme/carrier ratio was performed with each EziG™. In total, six different w/w ratios were tested (1:1, 1:3, 1:6, 1:9, 1:12, and 1:15), with an immobilization incubation

time of 1 h (Figure SI 3). After measurement of the remaining protein concentration in solution, 50 % of the protein immobilization could be determined with a 1:3 ratio. The immobilization rate could be increased up to 80 % with EziG™ OPAL with a 1:15 ratio, while 85 and 88 % protein immobilization could be respectively obtained with EziG™ CORAL and AMBER. However, no significative evolution could be observed between the ratios 1:9 and 1:15. To reduce the amount of carrier used to set up the processes, the 1:3 ratio was selected. As described later in this study, this ratio was found sufficient to complete the transamination step in only 4 h. The immobilization incubation time was also verified. Protein immobilization rates were measured with the three carriers and a 1:3 ratio, over 3 h (Figure SI 4). No significative evolution could be observed after 60 min of incubation for the EziG™ OPAL, with 60 % maximum protein loading. For the EziG™ CORAL and AMBER, the maximum protein loadings were 66 and 59 %, respectively, after 2 h. Based on these results, a 1:3 enzyme/carrier ratio was selected, with an incubation time of 1 h.

Following these preliminary experiments, the activities of *Cv*-TA@EziG™ OPAL, CORAL, and AMBER were measured with **4a** as the acceptor and alanine as donor, to select the best carrier for the process. The reaction advancement was followed spectrophotometrically and the conversion of **4a** into **4b** was confirmed by HPLC. The best carrier was EziG™ OPAL, with 61 % conversion of **4a** into **4b** in 60 min (Figure SI 5). Interestingly, this yield, corresponding to the one measured during the thermoactivity assays with alanine, was reached after 30 min of reaction. EziG™ AMBER and CORAL both reached 46 % conversions in 60 min and only 35 % in 30 min. Based on these results, the activity of *Cv*-TA@EziG™ OPAL was tested at 60 °C under the previously used conditions. In this case, only 37 % conversion was achieved after 60 min (Figure SI 6). In fact, 34 % conversion of **4a** was observed after the first 10 min of reaction but no further conversion was observed thereafter. This confirms the instability of *Cv*-TA at this temperature and demonstrates that its immobilization on the EziG™ carrier materials does not help protect the enzyme from denaturation.

Having achieved the best conversion yields with the EziG™ OPAL carrier, the recyclability of *Cv*-TA@EziG™ OPAL was also tested. MBA in a 1:1 ratio was this time used as donor to mimic the final conditions of the hybrid process. As expected, 100 % conversion was measured after 5 h of reaction during the first cycle (Figure SI 7). The second transamination cycle was performed after the *Cv*-TA@EziG™ OPAL was kept at 4 °C for 16 h. This time, only 30 % conversion was achieved in 5 h, and full conversion could be obtained after 24 h. This shows the instability of *Cv*-TA, even when immobilized on the EziG™ OPAL carrier. A last cycle was performed right after the second transamination cycle. This time, 13 % conversion was achieved in 5 h, and full conversion could be obtained after 72 h. Consequently, the immobilization of *Cv*-TA on EziG™ OPAL is only advantageous for the easy removal of the catalysts and a simplified purification of the reaction products.

In conclusion of this part of the study, EziG™ OPAL was selected as the carrier for the transaminase immobilization for further use in the hybrid process. Considering the significant loss in the *Cv*-TA@EziG™ OPAL activity at 60 °C, a temperature of 30 °C was selected as the optimal temperature for the transamination step in the final hybrid process for the production of **4b**. Because the selected chemocatalyst was effective at 60 °C, the process was performed as a one-pot/two-steps reaction with a short cool down between the two reaction steps. Under these conditions, no recycling of the catalysts was expected. However, the use of heterogeneous catalysts still eases the purification of the products.

One-pot/two-steps heterogeneous hybrid reaction

According to the optimization studies, the best chemocatalyst selected for the production of **4a** from **1a** and the immobilized enzyme effective for the subsequent conversion of the latter into **4b**, were employed in a one-pot/two-steps heterogeneous hybrid reaction. According to the previous results, this reaction was set up as follows in 10 mL total reaction volume (Figure 5): the first step was performed in sodium phosphate buffer (pH 8) at 60 °C using the Pt/SiO_2 catalyst. This step led to the production of **4a** from **1a**. After complete conversion of **1a**, the reaction mixture was cooled down to 25 °C and *Cv*-TA@EziG™Opal was added to the suspension together with *(S)*-MBA as the amine donor and PLP. After complete conversion of **4a** into **4b**, the products were purified and characterized.

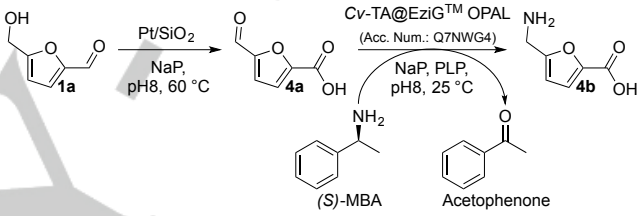

Figure 5. One-pot/two-steps hybrid heterogeneous catalytic process for the conversion of 5-hydroxymethylfurfural (HMF) into *5*-aminomethyl-*2*-furancarboxylic acid (AMFC), combining a Pt/SiO_2 chemocatalyst and *Chromobacterium violaceum* transaminase (*Cv*-TA). The first step was performed in sodium phosphate buffer, at pH 8 and 60 °C, on **1a** with Pt/SiO_2 as the catalyst. Once **1a** was entirely converted, the second step was initiated after a short cool down period at room temperature (25 °C) and performed with the addition of Cv-TA@EziG™ OPAL, the amine donor *(S)*-methylbenzylamine (MBA), and pyridoxal phosphate (PLP). This second step was then carried out in the same reaction mixture at 30 °C until complete conversion of **4a** into **4b** was attained.

Interestingly, complete conversion of **1a** was only observed after 48 h (Figure 6), despite the gas phase volume being proportionally identical to that used during the chemocatalyst screening step. However, in the case of the one-pot/two-steps reaction, the reaction volume was set to 10 mL to allow for more sampling, and considering the simple rotative agitation used, this scale factor may have induced a change in catalysts mixing, resulting in kinetics variations. Additionally, small amount of **3a** could be detected during the reaction, with maximum of 0.9 mM (9 %) after 24 h of reaction, and was found completely consumed after 64 h. At this, only **4a** and **5a** were remaining in the reaction mixture, with 5.2 mM and 4.8 mM respectively. The transamination step was consequently initiated. After 4 h at 25 °C, complete conversion of **4a** into **4b** could be observed according to the previous transamination syntheses. After the

transamination step, a yield of 53 % **4b** was obtained, with a final yield of 50 % after the purification step.

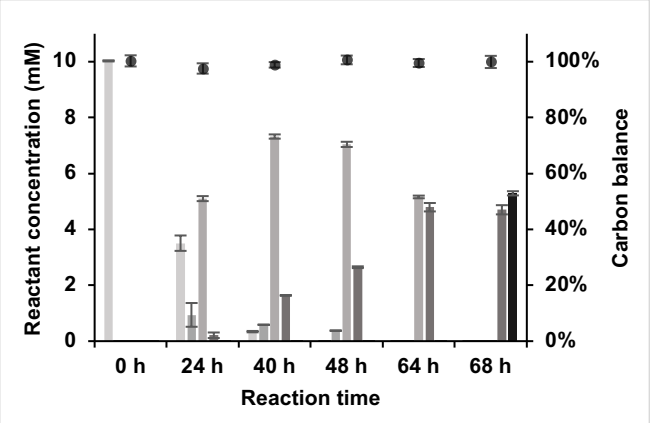

Figure 6. Concentrations of **1a**, **3a**, **4a**, **5a**, and **4b** measured by high-performance liquid chromatography with diode-array detection (HPLC-DAD) after 0, 24, 40, 48, 64, and 68 h. The first oxidative chemocatalytic step was performed at 60 °C for 64 h in 10 mL sodium phosphate buffer at pH 8, on 10 mM **1a** and 20 mg Pt/SiO_2 (1/20 substrate/metal ratio). The mixture was then cooled to 25 °C and 10 mg of *Cv*-TA@EziG™ OPAL were added with 1 mL of 100 mM *(S)*-methylbenzylamine (MBA) and 500 µM pyridoxal phosphate (PLP) solution in ultra-pure water (10 mM and 50 µM final concentrations, respectively). The transamination was run over 4 h. Carbon balances (•) were calculated for each reaction time based on the average measured reactant concentrations.

Despite succeeding in the production of the desired **4b** product, with only **5a** as major impurity, according to the results obtained, it appeared to be possible to optimize the final **4b** yield by performing the transamination step earlier. A second experiment was consequently carried out in the same condition, and the transamination step was performed after 48 h where **4a** concentration was found at its maximum with 7.7 mM (77 %) produced (Figure SI 26). In this case, a complete conversion of **4a** into **4b** could again be observed, with a final yield of 77 % in **4b**. The **5a** final concentration was consequently found lower than during the first experiment with 21 % yield. The transamination step being performed earlier, a small quantity of **3a** could also be detected after the transamination step (1 %). This impurity could easily be removed from the two major products during the purification step, and a final yield of 67 % and 20 % could be recovered in **4b** and **5a**, respectively.

A third experiment, identical to the second one, was then performed to evaluate the possibility of using IPA instead of MBA as donor. As stated earlier, a 10:1 donor/acceptor ratio was used in this case, and a quantitative conversion of **4a** into **4b** was also observed in 4 h of transamination step (Figure SI 30). Notably, the same product profile was observed at each reaction time, while the FDCA concentration was slightly higher after 48 h, with 2.4 mM produced. Finally, 6.7 mM (67 %) **4b** and 2.7 mM (27 %) **5a** could be obtained. As observed previously, only 1 % **3a** was detected at the end of the process. After purification, yields of 57 % **4b** and 20 % **5a** could be recovered.

With a complete consumption of **1a** in 48 h, this result represents the first methodology ever described for the synthesis of **4b** in a one-pot/two-steps process from this precursor. Notably, the overall yield obtained in 52 h of reaction (77 %) was substantially higher than that described by Dunbabin *et al.*, with MBA for the transamination step with *Cv*-TA (47 %) on one hand, but also with a more conventional organic synthesis approach (60 %) on the other hand. IPA could also be successfully used as amine donor for the process, with complete conversion of **4a** into **4b** in 4 h. This confirms that this approach represents an efficient way to synthetize **4b**. Additionally, the first reaction led to the production of 4.7 mM (47 %) **5a** as unique secondary product during the first experiment. While not being optimized in this objective, this new process could also represent an efficient way to produce **5a**, which remains one of the most interesting derivatives from **1a** as it can be used to produce another highly industrially valuable biobased polymer, the polyethylene furanoate (PEF). Particularly, as compounds **4b** and **5a** can be easily separated from each other by a simple liquid/liquid phase extraction process.

Conclusion

Briefly, we herein report the successful first one-pot/two-steps fully heterogeneous hybrid catalytic process for the direct production of AMFC from HMF. Among the 15 metal chemocatalysts tested, Pt/SiO_2 proved to be the most effective to convert HMF into AFCA, with 81 % yield in only 24 h, at 60 °C, in sodium phosphate buffer (pH 8). In parallel, *Cv*-TA was found to be efficient for the complete conversion of AFCA into AMFC in 4 h, at 30 °C, in sodium phosphate buffer (pH 8). To set up a fully heterogeneous process and aid product purification, the possibility of immobilizing the *Cv*-TA on EziG™ carrier was also studied. EziG™ OPAL material was found to be the best carrier, with almost full retention and maintenance of the *Cv*-TA activity at 30 °C in sodium phosphate buffer (pH 8). However, the immobilized enzyme could not be recycled over several synthesis cycles with already 70 % activity decrease during the second cycle. The combination of these two catalysts into a one-pot/two-steps process was successfully implemented with a maximum yield of 77 % in AMFC, and 67 % yield in product recovered after the purification step. To the best of our knowledge, this represents the highest yield ever reported for the production of AMFC through a catalytic process. Additionally, this process led to the formation of FDCA as major byproduct in all cases, which can easily be separated from AMFC by simple liquid/liquid extraction. This second compound serves, along with ethylene glycol, as a precursor for the synthesis of PEF, a new biobased polymer with industrial processes being currently validated for its high-scale production.

Experimental Section

Generalities

All chemicals were obtained from chemical suppliers and used as received unless otherwise stated. All the products were supplied by Sigma-Aldrich (Switzerland): *5*-hydroxymethylfurfural, *5*-aldehyde-*2*-furancarboxylic acid, *5*-hydroxymethyl-*2*-furancarboxylic acid, *2,5*-dicarboxaldehydefuran, furan dicarboxylic acid, lactate dehydrogenase from rabbit muscle (EC 1.1.1.27; LDH), nicotinamide adenine dinucleotide, *3*-trimethylsilyl-*2,2,3,3*-tetradeuteropropionate, deuterium oxide, isopropylamine, pyridoxal phosphate, sodium phosphate monobasic, l-alanine, *(S)*-*α*-methylbenzylamine, Bradford reagent, DOWEX 50WX8 100–200 mesh ion exchange resin, ammonium hydroxide solution (30 %), and Luria-Bertini broth. All analytical solvents were of HPLC/MS grade.

Spectrophotometric measurements were performed on a Spectramax i3 (Molecular Devices, USA).

NMR analysis

^{1}H and ^{13}C NMR spectra were recorded at 25 °C using a Bruker Advance 300 spectrometer (Bruker, USA). The coupling constants were measured in Hertz (Hz) and multiplicities for ^{1}H NMR coupling were presented as *s* (singlet), *d* (doublet), *t* (triplet), and *m* (multiple). The chemical shift was presented relative to the sodium trimethylsilyl propanoate reference.

HPLC analysis

The reaction product analyses were performed on an Ultra-fast HPLC-DAD-MS–LCMS-2020 (Shimadzu, Japan), using a Brownlee Spheri-5 RP-18 (4.6 x 250 mm) cartridge column. Injection volumes of 10 µL were used for all the samples. The water and acetonitrile elution phases contained 0.1 % trifluoroacetic acid (TFA). Elution was carried out at 0.5 mL.min^{-1}, with a 30 °C oven temperature for the column. The elution profile was as follows: 15 min of 100 % water phase, followed by the progressive shifting of the water phase toward 100 % acetonitrile phase in 2 min. The 100 % acetonitrile phase was held for 2 min and then shifted again to 100 % water phase in 2 min. The 100 % water phase was held until the end of the run, with a total run time of 25 min, to equilibrate the column and attain a stable pressure for the next injection. The products were detected at three different wavelengths, namely 215, 245, and 280 nm. The reaction products were detected at the following retention times and wavelengths: **4b**: 8.2 min/245 nm, **1b**: 9.46 min/210 nm, **3a**: 12.2 min/245 nm, **4a**: 13.2 min/280 nm, **5a**: 13.8 min/245 nm, **1a**: 14.5 min/280 nm, and **2a**: 16.6 min/280 nm. The HPLC-DAD calibration curves of these compounds are illustrated in Figures SI 14, 13, 10, 11, 12, 8, and 9, respectively.

Chemocatalyst syntheses

The 15 catalysts described in this paper were synthetized using the following four different approaches according to the methods listed in Table 1:

Reduction-precipitation (C1, C7)

The chemical reduction of the catalyst with hydrazine was performed in deionized water in a 110 cm^3 three-necked reaction flask immersed in a thermostatic water bath. The reaction flask was fitted with a reflux condenser and a thermocouple to control the reaction temperature. A suspension of the gold precursor [tetrachloroauric (III) acid, Sigma Aldrich, <99 %] and the support (1 g Al_2O_3 in 60 cm^3 distilled water) was stirred for 0.5 h at room temperature. The reaction mixture was then heated slowly from 25 to 50 °C and 2 mL 80 % aqueous hydrazine (Sigma Aldrich, <99 %) was subsequently added (N_2H_4/H_2O ratio: 0.3/5). The pH of the solution was 12 and remained almost constant and the reaction was complete after 1 h. After reduction, the solid was filtered, washed with distilled water, and dried in air at 100 °C for 16 h. The final Au loading was determined by inductively coupled plasma-optic (ICP) emission spectroscopy (720-ES ICP-OES, Agilent, USA) with axial viewing and simultaneous CCD detection.

Sol immobilization (C2, C3, C4, C5, C6, C8, C11, C12)

A 2 wt.% solution of PVA was added to an aqueous $HAuCl_4$ solution ($5.08 \cdot 10^{-4}$ M) under vigorous stirring [PVA/Au (w/w) = 1.2]. A 0.1 M freshly prepared solution of $NaBH_4$ [$NaBH_4$/Au (mol/mol) = 5] was then added to form a light-red (Au) metallic sol. After 30 min of sol generation, the colloid was immobilized by adding the support (MgO, CaO, TiO_2, CeO_2, ZrO_2, and Amberlyst) under vigorous stirring. The amount of support was calculated to give a total final metal loading of 2 wt.% (nominal). After 2 h, the slurry was filtered and the solid was washed with hot deionized water (2 x 25 mL) and ethanol (2 x 25 mL) before drying at 100 °C for 1 h. The final metal loading was determined by ICP analysis.

Wet impregnation (C9, C10)

Pt/SiO_2: $Pt(NH_3)_4Cl_2$ and $Pt(NH_3)_4(OH)_2$ (0,565 and 0,502 mg respectively, molar ratio 1:1) salts were dissolved in 20 mL of deionized water. Silica (Degussa; specific surface area, 203 m^2.g^{-1}) was then added and the pH of the reactant mixture was maintained at 8.9. The mixture was mixed for 1 h at room temperature, filtered, and washed with hot water to remove all the Cl^- ions. The solid was then dried at 105 °C for 2 h and reduced with pure hydrogen at 420 °C for 4 h (2 °C.min^{-1} and 50 cm^3.min^{-1}). The final Pt loading was 6.3 %, as determined by ICP analysis

Ru/HAP: 0.059 mg of $Ru(acac)_3$ (acac, acetylacetinate; Sigma Aldrich <99 %) was mixed with HAP (1 g) in water (50 mL) for 1 h at RT. Next, the reactant mixture was evaporated on a rotary evaporator for 1 h. The obtained solid was calcined at 400 °C for 4 h (4 °C.min^{-1}) and the quantity of Ru was subsequently determined by ICP analysis.

Co-precipitation (C13, C14, C15)

$5.08 \cdot 10^{-4}$ M solutions of Au ($HAuCl_4$), Pt ($Pt(NH_3)_4Cl_2$), and Pd ($PdCl_2$) precursor were added dropwise to water solutions of the support (1 g in 50 cm^3 water) and the reactant mixtures were stirred at room temperature for 1 h. Next, a water solution of NaOH was added to reach pH 9. Finally, the solid was recovered by filtration, washed with water, and dried at 100 °C overnight. The solids were reduced with pure hydrogen at 300 °C for 4 h (2 °C.min^{-1} and 50 cm^3.min^{-1}).

Transaminase production

The transaminase from *Chromobacterium violaceum* (UniProt acc. num.: Q7NWG4), cloned in a pET-22b(+) plasmid and transformed into Escherichia coli BL21(DE3), was provided as isolated colonies on LB broth supplemented with 100 µg.mL^{-1} ampicillin on a petri dish by Professor Thierry Gefflaut, ICCF, Clermont-Ferrand, France. This enzyme was tagged with a 6-His tag at its N-terminal extremity. The original clone was created by Professor Veronique De Berardinis, Genoscope, Evry, France. A colony was picked and introduced in a 15-mL vial containing 5 mL sterile LB broth supplemented with 100 µg.mL^{-1} ampicillin. It was then incubated overnight (16 h) at 37 °C with 200 rpm agitation. Exactly 3 mL of this pre-inoculum was then introduced in 150 mL fresh LB broth supplemented with 100 µg.mL^{-1} ampicillin. The culture was incubated at 37 °C under 200 rpm agitation for 5 h and then supplemented with 0.5 mM isopropyl-β-d-thiogalactoside (IPTG) to induce enzyme overexpression. The culture was maintained at 30 °C overnight (16 h) under 200 rpm agitation and then centrifuged at 4,000 *g* for 10 min. Next, the supernatant was removed, and the pellet was washed twice with sodium phosphate buffer (40 mL, pH 7.0, 10 mM). The sample was centrifuged at 4,000 *g* for 10 min after each washing step and the supernatant was discarded. The resulting pellet was then resuspended in lysis sodium phosphate buffer (5 mL, pH 7.0, 10 mM; 50 µM pyridoxal phosphate). The cells were exploded with a French Press (FP) at 2.4 bar and the lysate was subsequently centrifuged at 16,000 *g* for 2 min to remove the cellular debris. The supernatant was recovered and stored at -80 °C before lyophilization. The protein concentration of the CFE was assayed using the Bradford methodology and was determined as ~10 mg.mL^{-1} protein for each enzyme production batch. Lyophilization, which was performed at room temperature under a pressure of 25 mBar, afforded a white powder.

Cv-TA/LDH enzymatic assay

All the assays were performed in triplicate. The reactions were implemented at 200-µL scale in a microtiter plater, using 100 mM sodium phosphate buffer (pH 8) containing 2 mM substrate [(**1a**), (**4a**), or (**2a**)], 5 U.mL^{-1} LDH, 0.5 mg.mL^{-1} NADH, 0.1 mM PLP, 0.1 mg.mL^{-1} *Cv*-TA CFE,

and 10 mM *l*-alanine. The kinetics were followed by spectrophotometry at 340 nm and 30 °C for 20 min. As described in the international measurement system, 1 UI enzyme activity corresponded to 1 µmol substrate transformed per minute. The optical path of the microtiter plate, well filled with 200 µL deionized water, was estimated at 0.59 cm.

AFCA transamination with Cv-TA using (S)-MBA as the amino donor

A 1 mL reaction mixture sample containing 10 mM **4a**, 100 mM sodium dihydrogen phosphate, 10 mM (*S*)-MBA, and 1 mM pyridoxal phosphate in ultra-pure water was adjusted to pH 8 using concentrated sodium hydroxide solution. Next, 1 mg.mL^{-1} Cv-TA CFE was added to the mixture and incubated for 5 h at 25 °C. A 50-µL aliquot was collected after 0.5, 1, 2, 3, 4, and 5 h, and product formation was quantified by HPLC-DAD at 245 and 280 nm as described in the general procedures.

AFCA transamination with Cv-TA using IPA as the amino donor

A 1 mL reaction mixture sample containing 10 mM **4a**, 100 mM sodium dihydrogen phosphate, 10 mM (or 1 M) IPA, and 1 mM pyridoxal phosphate in ultra-pure water was adjusted to pH 8 using concentrated sodium hydroxide solution. Next, 1 mg.mL^{-1} Cv-TA CFE was added to the mixture and incubated for 5 h at 25 °C. A 50-µL aliquot was collected after 0.5, 1, 2, 3, 4, and 5 h, and product formation was quantified by HPLC-DAD at 245 and 280 nm as described in the general procedures.

Cv-TA thermoactivity

The *Cv*-TA thermostability was tested at 30 and 60 °C. The reactions were implemented at 1-mL scale, using a 100 mM sodium phosphate buffer (pH 8) containing 4 mM of **4a**, 1 mM PLP, 25 mM *l*-alanine, and 0.1 mg.mL^{-1} *Cv*-TA CFE. The reactions were incubated on a dry bath at 30 and 60 °C and 20-µL aliquots were collected after 10, 20, 30, 60, and 90 min. Next, 20 µL of the 50 U.mL^{-1} LDH + 0.5 mg.mL^{-1} NADH and 160 µL of 100 mM sodium phosphate buffer (pH 8) were added to each aliquot after cool-down at room temperature. The NADH conversion was followed by spectrophotometry at 340 nm and 30 °C.

Protein loading evaluation on EziG^{TM}

EziG^{TM} OPAL, CORAL, and AMBER (EnginZyme, Sweden) were used as immobilization carriers for *Cv*-TA. Six different ratios (w/w 1:1, 1:3, 1:6, 1:9, 1:12, and 1:15) were tested. The desired carrier mass was suspended in 1 mL 100 mM sodium phosphate buffer (pH 8), containing 1 mg.mL^{-1} *Cv*-TA CFE and 1 mM PLP. The mixtures were incubated for 1 h at 25 °C on a rotative agitator (Tube Revolver, Thermoscientific, USA) at 22 rpm. The mixtures were then centrifuged at 16,000 *g* for 1 min and 15 µL of the supernatant was collected. The remaining protein concentration was measured using the Bradford assay at 595 nm and determined using a bovine serum albumin (BSA) calibration curve (0 to 1 mg.mL^{-1}; concentration step, 0.1 mg.mL^{-1}).

Enzyme loading incubation time optimization

EziG^{TM} OPAL, CORAL, and AMBER (EnginZyme, Sweden) were used as immobilization carriers for *Cv*-TA. Exactly 3 mg of each support was suspended in 1 mL 100 mM sodium phosphate buffer (pH 8), containing 1 mg.mL^{-1} *Cv*-TA CFE and 1 mM PLP. The mixtures were incubated for 3 h at 25 °C on a rotative agitator (Tube Revolver, Thermoscientific, USA) at 22 rpm. After 15, 30, 45, 60, 120, and 180 min the agitation was stopped and a 15 µL sample was collected from the aqueous phase. Each sample was kept in an ice bath before further analysis. The remaining protein concentration was measured using the Bradford assay at 595 nm and determined using a BSA calibration curve (from 0 to 1 mg.mL^{-1}; concentration step, 0.1 mg.mL^{-1}).

Cv-TA@EziG^{TM} activity measurement

EziG^{TM} OPAL, CORAL, and AMBER (EnginZyme, Sweden) were tested as immobilization carriers for *Cv*-TA. Thus, 1.5 mg of each support was suspended in 1 mL 100 mM sodium phosphate buffer (pH 8) containing 0.5 mg.mL^{-1} *Cv*-TA CFE and 1 mM PLP. The mixtures were incubated for 1 h at 25 °C on a rotative agitator (Tube Revolver, Thermoscientific, USA) at 22 rpm. The mixtures were then centrifuged at 16,000 *g* for 1 min and the supernatants were discarded. The beads (1 mL) were resuspended in 100 mM sodium phosphate buffer (pH 8) containing 0.1 mM PLP, 4 mM **4a**, and 25 mM *l*-alanine. The reaction mixtures were incubated for 90 min at 30 °C on a rotative agitator (Thermoscientific, USA) at 22 rpm. Next, 20-µL aliquots were collected after 10, 20, 30, 60, and 90 min, to which 20 µL of 50 U.mL^{-1} LDH + 0.5 mg.mL^{-1} NADH and 160 µL of 100 mM sodium phosphate buffer (pH 8) were added after cooling to room temperature. The disappearance of NADH was followed by spectrophotometry at 340 nm and 30 °C.

General synthetic Cv-TA@EziG^{TM} OPAL immobilization procedure

For the hybrid reactions, *Cv*-TA in CFE was immobilized on EziG^{TM} OPAL (EnginZyme, Sweden). Thus, 3 mg EziG^{TM} OPAL was suspended in 1 mL of 100 mM sodium phosphate buffer (pH 8) containing 1 mg.mL^{-1} *Cv*-TA CFE and 1 mM PLP. The mixture was incubated for 1 h at 25 °C on a rotative agitator (Thermoscientific, USA) at 22 rpm. The mixture was then centrifuged at 16,000 *g* for 1 min and the resultant supernatant was discarded. Cv-TA@EziG^{TM} OPAL beads were immediately used in the synthetic reaction to limit enzyme denaturation.

Recycling of Cv-TA@EziG^{TM} OPAL

Cv-TA was immobilized using the general synthetic procedure. The resulting *Cv*-TA@EziG^{TM} OPAL was then incubated in 1 mL of reaction mixture containing 10 mM **4a**, 100 mM sodium dihydrogen phosphate, 10 mM *(S)-α*-methylbenzylamine, and 1 mM pyridoxal phosphate in ultra-pure water. The mixture was incubated for 5 h at 25 °C on a rotative agitator (Tube Revolver, Thermoscientific, USA). Exactly 50 µL samples were collected after 30, 60, 120, 180, 240, and 300 min of reaction time, and the product concentrations were measured by HPLC-DAD at 245 and 280 nm. Once the reaction was complete (complete conversion of the substrate), the mixture was centrifuged at 16,000 *g* for 1 min and the supernatant was discarded. After the first cycle, the *Cv*-TA@EziG^{TM} OPAL was kept at 4 °C for 16 h. A fresh solution containing 10 mM **4a**, 100 mM sodium dihydrogen phosphate, 10 mM *(S)-α*-methylbenzylamine, and 1 mM pyridoxal phosphate in ultra-pure water was then added to the immobilized enzyme. Incubation was allowed to proceed over 24 h, as described previously, and the reaction products were quantified after 30, 60, 120, 180, 240, 300, and 1440 min. The mixture was then centrifuged at 16,000 *g* for 1 min and the supernatant was discarded. An identical reaction mixture was then added, as previously described, to the immobilized enzyme and the incubation was allowed to proceed over 72 h. The reaction products were finally quantified after 30, 60, 120, 180, 240, 300, and 4320 min.

Purification of the reaction products

All the amine products were purified on DOWEX 50WX8 100–200 mesh ion exchange resin with a ratio of 0.1 mmol product to 20 mL resin. The resin was first washed with ultra-pure water until a neutral pH was obtained. The reaction mixture was then directly deposited on the resin and washed with four volumes of ultra-pure water. Elution was initiated with 0.5 M ammonium solution in ultra-pure water until a basic pH was attained. The elution of the product was then completed with 1 M ammonium solution in ultra-pure water. The elution of the product, which was followed on TLC with 0.1 M ammonium solution in distilled water as the eluent, was revealed, using ninhydrin, as a yellow-brown spot. All the product-containing fractions were pooled together and evaporated using a MiVac Quattro Concentrator (Sp Scientific, United Kingdom) under 25 mBar at 35 °C.

FDCA was also purified on DOWEX 50WX8 100–200 mesh ion exchange resin with a ratio of 0.1 mmol product to 20 mL resin. The resin was first washed with ultra-pure water until a neutral pH was obtained. The reaction mixture was then directly deposited on the resin and washed with four volumes of ultra-pure water. The FDCA could directly be recovered after 20 mL of washing volume. Its elution was followed on TLC with 0.1 M ammonium solution in distilled water as the eluent, and the product was revealed by using a UV-lamp at 254 nm. All the product-containing fractions were pooled together. To ensure the absence of salts, the FDCA-containing solution (10 mL) was first acidified to pH 1 using a few drops of concentrated HCl and extracted using three aliquots of 20 mL ethyl acetate. The organic phase was finally evaporated using a MiVac Quattro Concentrator (Sp Scientific, United Kingdom) under 25 mBar at 35 °C.

Synthesis of the reference products

*5-Hydroxymethylfurfurylamine (HMFA, **1b**)*

A 10-mL reaction mixture sample containing 10 mM **1a**, 100 mM sodium dihydrogen phosphate, 10 mM *(S)-α*-methylbenzylamine, and 1 mM pyridoxal phosphate in ultra-pure water was adjusted at pH 8 using concentrated sodium hydroxide solution. Next, 10 mg lyophilized CFE was added and the reaction mixture was incubated for 4 h at 25 °C. The product formation was followed by ^{1}H NMR. After the reaction was complete, the product was obtained by purification on ion exchange resin as described in the general procedures (TLC: *Rf* = 0.79 / eluant: 0.1 M ammoniac in distilled water). After drying, the product was recovered with >99 % yield in the form of a yellowish-brown powder.

^{1}H NMR (D_2O, 300 MHz): 3.78 (2H, s, CH_2NH_2), 4.55 (2H, s, CH_2OH), 6.23 (1H, d), 6.35 (1H, d); ^{13}C (DEPT 45, D_2O, 300 MHz): 37.43, 55.78, 106.79, 109.06; ^{13}C (DEPT 135, D_2O, 300 MHz) 37.43, 55.78, 106.79, 109.06; HSQC (D_2O, 300 MHz): 3.78, 55.78 (CH_2OH); 4.55, 37.43 (CH_2NH_2); 6.23, 106.79; 6.35,109.06 (NMR spectra in Figures SI 15–18).

*5-Aminomethyl-2-furancarboxaldehyde (AMFA, **3b**)*

A 4-mL reaction mixture sample containing 10 mM ***2a***, 100 mM sodium dihydrogen phosphate, 10 mM *(S)-α*-methylbenzylamine, and 1 mM pyridoxal phosphate in ultra-pure water was adjusted to pH 8 using concentrated sodium hydroxide solution. Next, 4 mg lyophilized *Cv*-TA CFE was added, and the reaction mixture was incubated for 2 h at 25 °C. The product formation process was followed by HPLC-DAD and ^{1}H NMR over 2 h. The product could not be purified on ion exchange resin (TLC: *Rf* = 0.94 / eluant: 0.1 M ammoniac in distilled water).

*5-Aminomethyl-2-furancarboxylic acid (AMFC, **4b**)*

A 10-mL reaction mixture sample containing 10 mM **4a**, 100 mM sodium dihydrogen phosphate, 10 mM *(S)-α*-methylbenzylamine, and 1 mM pyridoxal phosphate in ultra-pure water was adjusted to pH 8 using concentrated sodium hydroxide solution. Next, 10 mg lyophilized CFE was added and the reaction mixture was incubated for 4 h at 25 °C. The product formation process was followed by ^{1}H NMR. After the reaction was complete, the product was obtained by purification on ion exchange resin as described in the general procedures (TLC: *Rf* = 0.85 / eluant: 0.1 M ammoniac in distilled water). After drying, the product was recovered in >99 % yield as a yellow powder.

^{1}H NMR (D_2O, 300 MHz): 4.29 (2H, s, C*H*2NH2), 6.64 (1H, d), 7.00 (1H, d); ^{13}C (DEPT 45, D_2O, 300 MHz): 38.41, 115.46, 118.63; ^{13}C (DEPT 135, D_2O, 300 MHz) 35.36, 112.52, 115.73; HSQC (D_2O, 300 MHz): 4.29, 38.41 (CH_2NH_2); 6.64, 115.46; 7.00,118.63 (NMR spectra described in Figures SI 19–22).

Catalyst screening for 5-hydroxymethylfurfural (1a) oxidation

The oxidation of **1a** was performed in a 2-mL GC vial. Thus, 2 mg solid catalyst was added to 1 mL of a 10 mM **1a** solution in 100 mM sodium phosphate buffer (pH 8) in ultra-pure water. The vials were incubated at 60 °C in a stove and stirred using a rotative agitator (Tube Revolver, Thermoscientific, USA) at 22 rpm, with an angle of 45° compared to the rotation axis to maintain good homogeneity in the reaction mixtures comprising the solid heterogeneous catalysts. In total, 15 different catalysts were tested as described in Table 1. A blank reaction was performed without the addition of a catalyst. To follow the product formation process, a 50-µL aliquot was collected after 24 h and analyzed by HPLC-DAD as described in the general procedures.

« One-pot/two-steps » reactions

The first one-pot/two-steps reaction was performed in a 20 mL vial. Exactly 20 mg of solid catalyst were added to 10 mL of a 10 mM **1a** solution in 100 mM aqueous sodium phosphate buffer at pH 8. The reaction mixture was incubated at 60 °C in a stove and stirred using a rotative agitator (Thermoscientific, USA) at 22 rpm. Aliquots (50 µL) were collected after 0, 24, 40, 48, and 64 h and the formation of the oxidation products was confirmed by HPLC-DAD. The reaction mixture was cooled down to room temperature (25 °C) after 64 h and 10 mg of *Cv*-TA@EziG^{TM} OPAL was then added to the solution together with 1 mL of 100 mM *(S)-α*-methylbenzylamine and 500 µM solution in ultra-pure water at pH 8. The reaction mixture was incubated at room temperature (25 °C) for 4 h. The product formation was confirmed by HPLC-DAD, as described in the general procedure after the reaction was complete. The reaction mixture was also analyzed by ^{1}H NMR to validate the complete conversion of **4a** into **4b** (Figure SI 23). After a total of 68 h of reaction, the catalysts were removed by centrifugation (4,000 *g*, 1 min) and the reaction products were purified on ion exchange resin as described in the general procedures. The *5*-aminomethyl-*2*-furancarboxylic acid was recovered as a yellowish powder, with a yield of 50 % (7.1 mg), and characterized by NMR (^{1}H, ^{13}C, and HSQC) and HPLC. The FDCA was recovered as a white powder, with a final yield of 43 % (6.7 mg) and confirmed by ^{1}H NMR and HPLC. In parallel to the synthesis, a blank reaction was run under the same conditions but in the absence of the Pt/SiO_2 catalyst. The second step was initiated after 70 h oxidation at 60 °C. The absence of oxidation of **1a** was followed by HPLC-DAD after 0, 24, 40, 48, 64, and 70 h (Figure SI 24), as described above, and the complete conversion of **1a** into **1b** after 4 h of transamination at 25 °C was confirmed in the same way (Figure SI 25).

For the second one-pot/two-steps reaction, oxidation step conditions were identical, and aliquots (50 µL) were collected after 0, 24, 40 and 48 h (Figure SI 26). Oxidation products formation was confirmed by HPLC-DAD. The reaction mixture was cooled down to room temperature (25 °C) after 48 h and the transamination step was performed under the same conditions as for the first one-pot/two-steps reaction. After 4 h incubation at 25 °C, the product formation was confirmed by HPLC-DAD as described in the general procedure. The reaction mixture was also analyzed by ^{1}H NMR to validate the complete conversion of **4a** into **4b** (Figure SI 27). The catalysts were removed as described before, and products were purified on ion exchange resin as described in the general procedures. After purification, **4b** and **5a** could be recovered with a final yield of 67 % (9.4 mg) and 20 % (3.1 mg) respectively. In parallel to this second reaction, the corresponding oxidation blank reaction was run under the same conditions but in the absence of the Pt/SiO_2 catalyst. The second step was initiated after 48 h oxidation at 60 °C. The absence of oxidation of **1a** was followed by HPLC-DAD after 0, 24, 40, 48 and 52 h (Figure SI 28), as described above, and the complete conversion of **1a** into **1b** after 4 h of transamination at 25 °C was confirmed in the same way (Figure SI 29).

For the third one-pot/two-steps reaction, oxidation step conditions were again identical to the two previous ones, and aliquots (50 µL) were collected after 0, 24, 40 and 48 h (Figure SI 30). Oxidation products formation was confirmed by HPLC-DAD. The reaction mixture was cooled to room temperature (25 °C) after 48 h and the transamination step was performed under the same conditions, as for the first one-pot/two-steps

reaction, with a 1M isopropylamine solution added instead of the 100 mM *(S)*-α-methylbenzylamine solution. After 4 h incubation at 25 °C, the product formation was confirmed by HPLC-DAD as described in the general procedure. The reaction mixture was also analyzed by ^{1}H NMR to validate the complete conversion of **4a** into **4b** (Figure SI 31). The catalysts were removed as described before, and products were purified on ion exchange resin as described in the general procedures. After purification, **4b** and **5a** could be recovered with a final yield of 57 % (8.1 mg) and 20 % (3.1 mg) respectively. In parallel to this third reaction, the corresponding oxidation blank reaction was run under the same conditions but in the absence of the Pt/SiO_2 catalyst. The second step was initiated after 48 h oxidation at 60 °C. The absence of oxidation of **1a** was followed by HPLC-DAD after 0, 24, 40, 48 and 52 h (Figure SI 32), as described above, and the complete conversion of **1a** into **1b** after 4 h of transamination at 25 °C was confirmed in the same way (Figure SI 33).

Acknowledgements

The authors would like to thank Prof. Thierry Gefflaut and Prof. Veronique De Beradinis for the Cv-TA expressing strain as well as Martine Sancelme for the protocol used for the enzyme overexpression. The authors would also like to acknowledge Dr. Till Bousquet and Celine Delabre for their help on the NMR structure determination of the amino products. The authors are grateful to Lenaick Herve for his participation in the production of the enzymes. They would also like to thank Dr. Svetlana Heyte, who handles the REALCAT platform where most of the experiments were performed. The HPLC-MS experiments were performed on the REALCAT platform funded by a French governmental subsidy managed by the French National Research Agency (ANR) within the frame of the "Future Investments' program (ANR-11- EQPX-0037). The Hauts-de-France region, FEDER, Ecole Centrale de Lille, and Centrale Initiatives Foundation are also warmly acknowledged for their financial contributions to the acquisition of REALCAT platform equipment. Finally, this study was supported by the French government through the Programme Investissement d'Avenir (I-SITE ULNE / ANR-16-IDEX-0004 ULNE) managed by the Agence Nationale de la Recherche.

Keywords: *5*-aminomethyl-*2*-furancarboxylic acid • *5*-hydroxymethylfurfural • biocatalysis • enzyme catalysis • heterogeneous catalysis • hybrid catalysis • platinum • transaminase

[1] P. Anastas, J. Warner, *Green Chemistry: Theory and Practice*, Oxford University Press, Oxford, New York, **2000**.

[2] a) S. Schmidt, K. Castiglione, R. Kourist, *Chem. - Eur. J.* **2018**, *24*, 1755–1768; b) N. Ríos-Lombardía, J. García-Álvarez, J. González-Sabín, *Catalysts* **2018**, *8*, 75; c) F. Rudroff, M. D. Mihovilovic, H. Gröger, R. Snajdrova, H. Iding, U. T. Bornscheuer, *Nat. Catal.* **2018**, *1*, 12–22; d) R. Bisogno, M. G. López-Vidal, G. de Gonzalo, *Adv. Synth. Catal.* **2017**, *359*, 2026–2049; e) H. Gröger, in *Cooperative Catalysis* (Ed.: R. Peters), Wiley-VCH Verlag GmbH & Co. KGaA, Weinheim, Germany, **2015**, pp. 325–350; f) H. Gröger, W. Hummel, *Curr. Opin. Chem. Biol.* **2014**, *19*, 171–179..

[3] a) O. Långvik, T. Saloranta, D. Y. Murzin, R. Leino, *ChemCatChem* **2015**, *7*, 4004–4015; b) C. A. Denard, H. Huang, M. J. Bartlett, L. Lu, Y. Tan, H. Zhao, J. F. Hartwig, *Angew. Chem., Int. Ed.* **2014**, *53*, 465–469.

[4] a) J. Zhao, B. R. Lichman, J. M. Ward, H. C. Hailes, *Chem. Commun.* **2018**, *54*, 1323–1326; b) M. J. Rodríguez-Álvarez, N. Ríos-Lombardía, S. Schumacher, D. Pérez-Iglesias, F. Morís, V. Cadierno, J. García-Álvarez, J. González-Sabín, *ACS Catal.* **2017**, *7*, 7753–7759; c) E. Liardo, N. Ríos-Lombardía, F. Morís, F. Rebolledo, J. González-Sabín, *ACS Catal.* **2017**, *7*, 4768–4774. d) R. C. Simon, E. Busto, J. H. Schrittwieser, J. H. Sattler, J. Pietruszka, K. Faber, W. Kroutil, *Chem. Commun.* **2014**, *50*, 15669–15672.

[5] a) A. Gimbernat, M. Guehl, N. Lopes Ferreira, E. Heuson, P. Dhulster, M. Capron, F. Dumeignil, D. Delcroix, J.-S. Girardon, R. Froidevaux, A. Gimbernat, M. Guehl, N. Lopes Ferreira, E. Heuson, P. Dhulster, M. Capron, F. Dumeignil, D. Delcroix, J.-S. Girardon, R. Froidevaux, *Catalysts* **2018**, *8*, 335; b) P. Schaaf, T. Bayer, M. Koley, M. Schnürch, U. T. Bornscheuer, F. Rudroff, M. D. Mihovilovic, *Chem. Commun.* **2018**, *54*, 12978–12981; c) H. Sato, W. Hummel, H. Gröger, *Angew. Chem., Int. Ed.* **2015**, *54*, 4488–4492; d) V. Gauchot, W. Kroutil, A. R. Schmitzer, *Chem. - Eur. J.* **2010**, *16*, 6748–6751.

[6] a) P. Zajkoska, M. Cárdenas-Fernández, G. J. Lye, M. Rosenberg, N. J. Turner, M. Rebroš, *Journal of Chemical Technology & Biotechnology* **2017**, *92*, 1558–1565; b) M. Sugiyama, Z. Hong, P.-H. Liang, S. M. Dean, L. J. Whalen, W. A. Greenberg, C.-H. Wong, *Journal of the American Chemical Society* **2007**, *129*, 14811–14817.

[7] F. Dumeignil, M. Guehl, A. Gimbernat, M. Capron, N. L. Ferreira, R. Froidevaux, J.-S. Girardon, R. Wojcieszak, P. Dhulster, D. Delcroix, *Catal. Sci. Technol.* **2018**, *8*, 5708–5734.

[8] R. Schoevaart, T. Kieboom, *Tetrahedron Lett.* **2002**, *43*, 3399–3400.

[9] M. Edin, J.-E. Bäckvall, A. Córdova, *Tetrahedron Lett.* **2004**, *45*, 7697–7701.

[10] M. Makkee, A. P. G. Kieboom, H. V. Bekkum, J. A. Roels, *J. Chem. Soc., Chem. Commun.* **1980**, 930–931.

[11] a) T. Xue, B. Peng, M. Xue, X. Zhong, C.-Y. Chiu, S. Yang, Y. Qu, L. Ruan, S. Jiang, S. Dubin, R. B. Kaner, J. I. Zink, M. E. Meyerhoff, X. Duan, Y. Huang, *Nat. Commun.* **2014**, *5*, 3200; b) Z. J. Wang, K. N. Clary, R. G. Bergman, K. N. Raymond, F. D. Toste, *Nat. Chem.* **2013**, *5*, 100–103; c) M. Filice, M. Marciello, M. del Puerto Morales, J. M. Palomo, *Chem. Commun.* **2013**, *49*, 6876–6878; d) K. Kamwilaisak, P. C. Wright, *Energy Fuels* **2012**, *26*, 2400–2406.

[12] B. H. Shanks, *ACS Chem. Biol.* **2007**, *2*, 533–535.

[13] a) S. Y. Lee, H. U. Kim, T. U. Chae, J. S. Cho, J. W. Kim, J. H. Shin, D. I. Kim, Y.-S. Ko, W. D. Jang, Y.-S. Jang, *Nat. Catal.* **2019**, *2*, 18–33; b) L. Wu, T. Moteki, A. A. Gokhale, D. W. Flaherty, F. D. Toste, *Chem* **2016**, *1*, 32–58; c) F. Dumeignil, M. Capron, B. Katryniok, R. Wojcieszak, A. Löfberg, J.-S. Girardon, S. Desset, M. Araque-Marin, L. Jalowiecki-Duhamel, S. Paul, *J. Jpn. Pet. Inst.* **2015**, *58*, 257–273; d) F. H. Isikgor, C. R. Becer, *Polym. Chem.* **2015**, *6*, 4497–4559; e) M. Dusselier, M. Mascal, B. F. Sels, in *Selective Catalysis for Renewable Feedstocks and Chemicals* (Ed.: K.M. Nicholas), Springer International Publishing, **2014**, pp. 1–40.

[14] R.-J. van Putten, J. C. van der Waal, E. de Jong, C. B. Rasrendra, H. J. Heeres, J. G. de Vries, *Chem. Rev.* **2013**, *113*, 1499–1597.

[15] a) S. Chen, R. Wojcieszak, F. Dumeignil, E. Marceau, S. Royer, *Chem. Rev.* **2018**, *118*, 11023–11117; b) R. Wojcieszak, C. Ferraz, J. Sha, S. Houda, L. Rossi, S. Paul, *Catalysts* **2017**, *7*, 352.

[16] a) W. Fan, C. Verrier, Y. Queneau, F. Popowycz, *Curr. Org. Synth.* **2019**, *16*, 583–614; b) L. Hu, L. Lin, Z. Wu, S. Zhou, S. Liu, *Renewable Sustainable Energy Rev.* **2017**, *74*, 230–257; c) A. A. Rosatella, S. P. Simeonov, R. F. M. Frade, C. A. M. Afonso, *Green Chem.* **2011**, *13*, 754.

[17] a) L. Hu, A. He, X. Liu, J. Xia, J. Xu, S. Zhou, J. Xu, *ACS Sustainable Chem. Eng.* **2018**, *6*, 15915–15935; b) M. M. Cajnko, U. Novak, M. Grilc, B. Likozar, *Biotechnol. Biofuels* **2020**, *13*, 66; c) B. Hočevar, M. Grilc, B. Likozar, *Catalysts* **2019**, *9*, 286.

[18] a) F. Drault, Y. Snoussi, S. Paul, I. Itabaiana, R. Wojcieszak, *ChemSusChem* **2020**, *13*, 5164–5172; b) R. Wojcieszak, I. Itabaiana, *Catal. Today* **2020**, *354*, 211-217.

[19] a) C. P. Ferraz, N. J. S. Costa, E. Teixeira-Neto, A. A. Teixeira-Neto, C. W. Liria, J. Thuriot-Roukos, M. T. Machini, R. Froidevaux, F. Dumeignil, L. M. Rossi, R. Wojcieszak, *Catalysts* **2020**, *10*, 75; b) C. P. Ferraz, M. Zieliński, M. Pietrowski, S. Heyte, F. Dumeignil, L. M. Rossi, R. Wojcieszak, *ACS Sust. Chem. Eng.* **2018**, *6*, 16332-16340; c) A. Roselli, Y. Carvalho, F. Dumeignil, F. Cavani, S. Paul, R. Wojcieszak, *Catalysts* **2020**, *10*, 73-84; d) J. Sha, S. Paul, F. Dumeignil, R. Wojcieszak, *RSC Adv.* **2019**, *9*, 29888-29901; e) C. P. Ferraz, A. S. Gabriel Marques, T.

Rodrigues Silva, P. H. Camargo, S. Paul, R. Wojcieszak, *Applied Sciences* **2018**, *8*, 1246-1257.

[20] a) S. Chen, C. Ciotonea, K. D. O. Vigier, F. Jérôme, R. Wojcieszak, F. Dumeignil, E. Marceau, S. Royer, *ChemCatChem* **2020**, *12*, 2050-2059; b) N. Capece, A. Sadier, C. P. Ferraz, J. Thuriot-Roukos, M. Pietrowski, M. Zieliński, S. Paul, F. Cavani, R. Wojcieszak, *Catalysis Science & Technology* **2020**, *10*, 2644-2651.

[21] F. Koopman, N. Wierckx, J. H. Winde, H. J. Ruijssenaars, *Bioresour. Technol.* **2010**, *101*, 6291-6296.

[22] W. P. Dijkman, D. E. Groothuis, M. W. Fraaije, *Angew. Chem. Int. Ed.* **2014**, *53*, 6515-6518.

[23] J. Carro, P. Ferreira, L. Rodríguez, A. Prieto, A. Serrano, B. Balcells, A. Ardá, J. Jiménez-Barbero, A. Gutiérrez, R. Ullrich, M. Hofrichter, A.T.Martínez, *FEBS J.*, **2015**, *282*, 3218-3229.

[24] Y. Z. Qin, Y. M. Li, M. H. Zong, H. Wu, N. Li, *Green Chem.* **2015**, *17*, 3718-3722.

[25] S. M. McKenna, S. Leimkühler, S. Herter, N. J. Turner, A. J. Carnell. *Green Chem.* **2015**, *17*, 3271-3275

[26] K. F. Wang, C. L. Liu, K. Y. Sui, C. Guo, C. Z. Liu. *ChemBioChem* **2018**, *19*, 654-659.

[27] V. Froidevaux, C. Negrell, S. Caillol, J.-P. Pascault, B. Boutevin, *Chem. Rev.* **2016**, *116*, 14181–14224.

[28] a) X. Chen, J. Wang, S. Huo, S. Yang, B. Zhang, H. Cai, *J. Therm. Anal. Calorim.* **2019**, *135*, 3153–3164; b) K. Krishnamoorthy, D. Subramani, N. Eeda, A. Muthukaruppan, *Polym. Adv. Technol.* **2019**, *30*, 1856–1864.

[29] a) M. S. Holfinger, A. H. Conner, D. R. Holm, C. G. Hill, *J. Org. Chem.* **1995**, *60*, 1595–1598; b) J. L. Cawse, J. L. Stanford, R. H. Still, *Die Makromolekulare Chemie* **1984**, *185*, 697–707.

[30] M. Chatterjee, T. Ishizaka, H. Kawanami, *Green Chem.* **2016**, *18*, 487–496.

[31] G. Chieffi, M. Braun, D. Esposito, *ChemSusChem* **2015**, *8*, 3590–3594.

[32] a) S. Jiang, C. Ma, E. Muller, M. Pera-Titus, F. Jérôme, K. De Oliveira Vigier, *ACS Catal.* **2019**, *9*, 8893–8902; b) G. Hahn, P. Kunnas, N. de Jonge, R. Kempe, *Nat. Catal.* **2019**, *2*, 71–77; c) X. Wang, W. Chen, Z. Li, X. Zeng, X. Tang, Y. Sun, T. Lei, L. Lin, *J. Energy Chem.* **2018**, *27*, 209–214; d) D. Chandra, Y. Inoue, M. Sasase, M. Kitano, A. Bhaumik, K. Kamata, H. Hosono, M. Hara, *Chem. Sci.* **2018**, *9*, 5949–5956; e) F. Blume, M. Albeiruty, J. Deska, *Synthesis* **2015**, *47*, 2093–2099; f) Z. Xu, P. Yan, W. Xu, S. Jia, Z. Xia, B. Chung, Z. C. Zhang, *RSC Adv.* **2014**, *4*, 59083–59087; g) M. A. Ayedi, Y. Le Bigot, H. Ammar, S. Abid, R. E. Gharbi, M. Delmas, *J. Soc. Chim. Tunis.* **2012**, 109–116.

[33] A. Dunbabin, F. Subrizi, J. M. Ward, T. D. Sheppard, H. C. Hailes, *Green Chem.* **2017**, *19*, 397–404.

[34] a) R. C. Simon, N. Richter, E. Busto, W. Kroutil, *ACS Catal.* **2014**, *4*, 129–143; b) S. Mathew, H. Yun, *ACS Catalysis* **2012**, *2*, 993–1001; c) M. Höhne, U. T. Bornscheuer, *ChemCatChem* **2009**, *1*, 42–51.

[35] A. Petri, G. Masia, O. Piccolo, *Catal. Commun.* **2018**, *114*, 15–18.

[36] a) T. K. Chakraborty, S. Tapadar, S. Kiran Kumar, *Tetrahedron Lett.* **2002**, *43*, 1317–1320; b) M. Sharma, P. Kumar, H. Singh, T. K. Chakraborty, *J. Mol. Struct.: THEOCHEM* **2006**, *764*, 109–115.

[37] a) F. Grasset, P. Rey, V. Bellière-Baca, M. Araque, S. Paul, F. Dumeignil, R. Wojcieszak, B. Katryniok, *Catal. Today* **2017**, *279*, 164–167; b) R. Wojcieszak, I. M. Cuccovia, M. A. Silva, L. M. Rossi, *J. Mol. Catal. A: Chem.* **2016**, *422*, 35–42; c) V. G. Baldovino-Medrano, G. Pollefeyt, V. Bliznuk, I. Van Driessche, E. M. Gaigneaux, P. Ruiz, R. Wojcieszak, *ChemCatChem* **2016**, *8*, 1157–1166.

[38] M. D. Truppo, J. D. Rozzell, J. C. Moore, N. J. Turner, *Org. Biomol. Chem.* **2009**, *7*, 395–398.

[39] K. E. Cassimjee, M. Kadow, Y. Wikmark, M. S. Humble, M. L. Rothstein, D. M. Rothstein, J.-E. Bäckvall, *Chem. Commun.* **2014**, *50*, 9134–9137.

[40] M. P. Thompson, S. R. Derrington, R. S. Heath, J. L. Porter, J. Mangas-Sanchez, P. N. Devine, M. D. Truppo, N. J. Turner, *Tetrahedron* **2019**, *75*, 327–334.

Entry for the Table of Contents

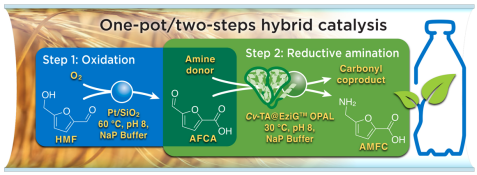

5-Hydroxymethylfurfural is one of the main building blocks that can be easily obtained from biomass. Among its many possible transformations, furfurylamines have been little explored, probably due to their difficult synthesis which generally requires difficult conditions. This study presents a hybrid catalytic system combining a metal nanoparticle and an enzyme to efficiently produce *5*-aminomethyl-*2*-furancarboxylic acid under mild conditions.

5-aminomethyl-*2*-furancarboxylic acid • *5*-hydroxymethylfurfural • hybrid catalysis • platinum • transaminase